

Article

Biomechanical and Histological Analysis of Titanium (Machined and Treated Surface) Versus Zirconia Implant Materials: An In Vivo Animal Study

Sergio Alexandre Gehrke ^{1,2,3,*}, Juan Carlos Prados-Frutos ^{4,†}, María Prados-Privado ⁵, José Luis Calvo-Guirado ², Jaime Aramburú Júnior ⁶, Leticia Pérez-Díaz ⁷, Patricia Mazón ³, Juan Manuel Aragonese ⁸ and Piedad N. De Aza ³

¹ Department of Research, Biotecnos, Cuareim 1483, Montevideo CP 11100, Uruguay

² Department of Oral and Implant Surgery, Faculty of Health Sciences, Universidad Católica de Murcia (UCAM), 30107 Murcia, Spain; jlcalvo@ucam.edu

³ Instituto de Bioingeniería, Universidad Miguel Hernández, Avda. Ferrocarril s/n/, 03202 Elche (Alicante), Spain; pmazon@umh.es (P.M.); piedad@umh.es (P.N.D.A.)

⁴ Department of Medicine and Surgery, Faculty of Health Sciences, Rey Juan Carlos University, 28922 Madrid, Spain; juancarlos.prados@urjc.es

⁵ Department of Continuum Mechanics and Structural Analysis, Carlos III University, 28911 Madrid, Spain; mprados@ing.uc3m.es

⁶ Department of Surgery, Faculty of Veterinary, Faculty of Itapiranga, Itapiranga CP 89896000, Brazil; jaimearamburujunior@gmail.com

⁷ Laboratorio de Interacciones Molecular, Facultad de Ciencias, Universidad de la Republica, Calle Iguá 4225, Montevideo 11400, Uruguay; letiperez@gmail.com

⁸ Department of Dental Research, Universidad Federico Henríquez y Carvajal (UFHEC), Santo Domingo 10107, Dominican Republic; jaragonese@ufhec.edu.do

* Correspondence: sergio.gehrke@hotmail.com; Tel./Fax: +598-2901-5634

† Equal Contribution.

Received: 11 February 2019; Accepted: 12 March 2019; Published: 14 March 2019



Abstract: Objectives: The aim of this study was to perform an in vivo histological comparative evaluation of bone formation around titanium (machined and treated surface) and zirconia implants. For the present study were used 50 commercially pure titanium implants grade IV, being that 25 implants with a machined surface (TiM group), 25 implants with a treated surface (TiT group) and, 25 implants were manufactured in pure zirconia (Zr group). The implants ($n = 20$ per group) were installed in the tibia of 10 rabbits. The implants distribution was randomized ($n = 3$ implants per tibia). Five implants of each group were analyzed by scanning electron microscopy and an optical laser profilometer for surface roughness characterization. Six weeks after the implantation, 10 implants for each group were removed in counter-torque for analysis of maximum torque value. The remaining samples were processed, included in historesin and cut to obtain non-decalcified slides for histomorphological analyses and histomorphometric measurement of the percentage of bone-implant contact (BIC%). Comparisons were made between the groups using a 5% level of significance ($p < 0.05$) to assess statistical differences. The results of removal torque values (mean \pm standard deviation) showed for the TiM group 15.9 ± 4.18 N cm, for TiT group 27.9 ± 5.15 N cm and for Zr group 11.5 ± 2.92 N cm, with significant statistical difference between the groups ($p < 0.0001$). However, the BIC% presented similar values for all groups (35.4 ± 4.54 for TiM group, 37.8 ± 4.84 for TiT group and 34.0 ± 6.82 for Zr group), with no statistical differences ($p = 0.2171$). Within the limitations of the present study, the findings suggest that the quality of the new bone tissue formed around the titanium implants present a superior density (maturation) in comparison to the zirconia implants.

Keywords: osseointegration; bone healing; bone quality; zirconia implants; titanium implants

1. Introduction

Titanium implants have become a common practice for replacing missing teeth. Although zirconia implants are gaining ground in clinical practice. They are not yet a clinical routine due to the lack of scientific and mechanical studies [1,2], although in the last few years, zirconia implants have been studied in detail as alternative biomaterials for replacement of missing teeth [3].

A large percentage of zirconium implants are formed by a tetragonal zirconium polycrystalline 3 molar (3Y-TZP). It has been demonstrated that this configuration does not cause an inflammatory reaction, no adhesion of proteins, adherence of cells osteoblásticas, cell adhesion, cell differentiation binding occurs implant and especially titanium [2].

Titanium and zirconia differ in many aspects and have their own advantages and disadvantages. Zirconia (ZrO_2) is a polycrystalline ceramic dioxide of the transition metal zirconium (Zr) [4]. The advantages of zirconia are its low modulus of elasticity and thermal conductivity, low affinity to plaque, low corrosion and high biocompatibility [5], in addition to its white color. Many studies have found zirconia Young's modulus between 200 and 210 GPa [6]. Zirconia has also less bacterial adhesion in the surface than titanium, therefore, biologic complications should be reduced [7]. However, the main disadvantage of zirconia implants is the low-temperature degradation (ageing) which results in degradation of the mechanical properties (strength, toughness and density of the material) [8,9]. Another important factor is that zirconia is more brittle and more vulnerable by bending and crack growth [10], so fracture resistance of zirconia dental implants is worse than titanium implants [11]. Due to its advantages, zirconia is becoming a material of great interest for dentistry, particularly where aesthetics are required [3].

Several in vitro studies have investigated the biocompatibility of zirconia and its osseointegration with the conclusion that it promotes proliferation of osteoblasts at levels greater than aluminum oxide [4,12]. Other studies have shown that zirconia implants reduce bacterial colonization, and therefore, the risk of periimplantitis [13]. Biocompatibility has been also proven in several animal investigations [14,15]. Osseointegration of zirconia implants has been demonstrated in several in vivo experiments where the conclusion was that that osseointegration is comparable to the level achieved with titanium alloys [16,17].

Ceramic materials, as zirconia, have an important sensitivity to surface defects which may generate cracks. These cracks can penalty the mechanical properties of zirconia dental implants [18]. Due to the mechanical properties of titanium and zirconia are different, usual geometries employed in titanium implants cannot be transferred to zirconia designs [19]. Zirconia is sensitive to subcritical crack growth and bending, so sharp edges, as common in titanium implants, should be avoided [19,20]. For this reason, most zirconia dental implants are one-piece or two-piece systems with a bonded abutment [5].

The main inconvenience of employing a two-piece implant with the abutment bonded to the implant is that, in case of failure, the entire implant must be removed. Some screwed implant-abutment connections have been developed with the aim of reducing these limitations [5,21]. Some in vitro studies have concluded that the geometry of implant-abutment connection has a crucial influence of zirconia abutments behavior [22]. Failures in two-piece systems always involve the connecting screw because zirconia does not tolerate tensile forces, which appear around the screw [23]. In addition, zirconia is sensitive to ageing in the presence of water, which is an oral environment is crucial because this ceramic will become a brittle behavior [1].

There is an interest in the use of zirconia in dental implants due to the increase in the number of published studies in the last few years on this topic [24]. However, limited in vivo and in vitro research data are available regarding the performance of zirconia for dental applications.

Thus, the aim of this study was to compare the performance of aspects related to osseointegration (biomechanics and histologic aspects) of titanium (machined and treated surface) versus zirconia implants inserted in tibias of rabbits after a period of 6 weeks.

2. Materials and Methods

Animals and experimental groups: Ten New Zealand adult female rabbits with a mean weight of 4.0 kg, were used in this study. The experiment was performed in accordance with the Brazilian guidelines and regulations, i.e., followed the standards of animal welfare in accordance to the Sociedade Brasileira de Ciência de Animal de Laboratório”, SBCal (<http://www.cobea.org.br>) and the Brazilian federal law regulating the issues related to animal research that was published in October 2008 (http://www.planalto.gov.br/ccivil_03/_Ato2007-2010/2008/Lei/L11794.htm). The study was approved by the ethics committee of the Veterinary Medicine of the Faculty of Itapiranga (Itapiranga, Brazil-#004-09-2015), and the animals received all the care stipulated by the institution.

Sixty special mini-implants with 2.2 mm in diameter and 4 mm in length were manufactured specially for this study by Implacil De Bortoli Company (São Paulo, Brazil) in two different materials. The implants were divided into three groups ($n = 25$ per group): two titanium groups, where the implants manufactured in commercially pure titanium grade IV, which 25 implants were machined (TiM group) and a smooth surface was obtained (Figure 1a), and 25 implants were the surface was treated (TiT group) with sandblasted acid-etched using TiO_2 particles with 100 μm to blasting and maleic acid to the conditioning (Figure 1b); Zr group, where the implants were produced in yttrium-stabilized tetragonal zirconia polycrystal (Y-TZP), which was standardized from CAD-CAM blocks (Figure 1c). Then, the specimens were treated, sterilized and packed using the same protocol standardized by the implants commercialized in the market.

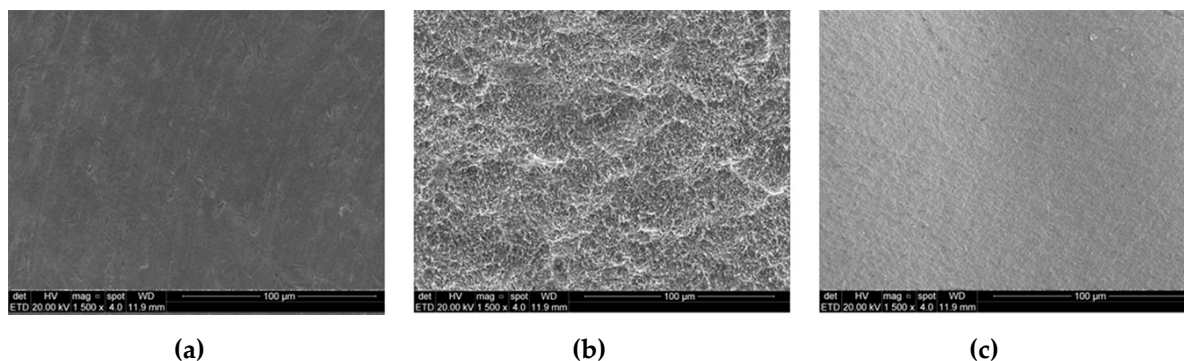


Figure 1. Scanning Electronic Microscopy images of the implant surface of (a): TiM group, (b): TiT group and (c): Zr group, respectively. The increase of $1.500\times$.

Implants characterization: A profiler software (Leica DCM 3D Dual Core, version for Windows, Leica Microsystems Ltd., Heerbrugg, Switzerland) calculated the surface roughness parameters S_a and R_a . S_a measurement was performed in the total area ($254.64 \times 190.90 \mu\text{m}^2$) and R_a was measured in a length of 254.64 μm . The mean of roughness values of S_a and R_a and standard deviation were calculated from the five profiles of each specimen group. The meaning of the surface roughness parameters S_a and R_a .

A roughness value can either be calculated on a profile (line) or on a surface (area). R_a is the parameter of the profile roughness parameter, which is the most employed, and S_a is a measure of area roughness. R_a means the value obtained by the following formula and expressed in micrometer (μm) when sampling only the reference length from the roughness curve in the direction of the mean line, taking x -axis in the direction of mean line and y -axis in the direction of longitudinal magnification of this sampled part and the roughness curve is expressed by $y = f(x)$ (Figure 2):

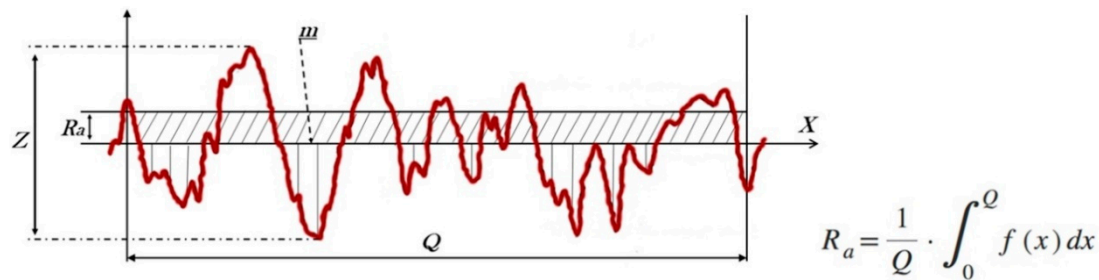


Figure 2. Representative scheme of the parameters measurement (S_a , R_a and Z) on the surface samples and the arithmetic average roughness calculation of the R_a .

S_a is the extension of R_a (arithmetical mean height of a line) to a surface. It expresses, as an absolute value, the difference in height of each point compared to the arithmetical mean of the surface. This parameter is used generally to evaluate surface roughness. Moreover, the longest distance recorded among the peak and valley, high variation of the valleys (Z parameter) was analyzed.

After the surface analysis, they were coated with a gold sputter (SCD 050; Bal-Tec RG, Balzers, Liechtenstein, Germany) and the surface morphology was observed on SEM (XL30 FEG; Philips, Eindhoven, The Netherlands) with the magnification of $1500\times$.

Surgical procedure: Initially the animals were pre-anesthetized intramuscularly with a dose of acepromazine maleate (0.2 mg/kg) and morphine sulfate (2 mg/kg and, then, ketamine chloride (10 mg/kg) and 1 mg midazolam (1 mg/kg) were administered intravenously under general anesthesia. Additionally, 1 mL of local anesthetic (3% Prilocaine-felypressin, Astra, Mexico) was subcutaneously injected at the site of surgery to improve analgesia and control bleeding. The trichotomy in both tibias and antisepsis with topical iodopovidone were performed.

The incision was 10 mm below the articulation in the skin and posteriorly in the fascia in the proximal-distal direction. Three perforations were made using a pilot spade drill with 2 mm in diameter and 5 mm in length with copious irrigation using saline solution. A distance of 10 mm between the three perforations was maintained. Then, the implants were manually installed at the bone level, with the hexagonal portion of the implant head out of the bone (Figure 3), controlled by an experienced surgeon (SAG). The animals were divided into 2 groups of 5 animals, for biomechanical test and histological analysis. Then, the implants were distributed by a randomized protocol (www.randomization.com) inside of the two lots ($n = 3$ implants per tibia). The suture was performed in two planes (muscular and subcutaneous) using a simple point, with nylon 4-0 (Johnson & Johnson/Ethicon, New Brunswick, NJ, USA).



Figure 3. Representative image of the implant samples installed in an animal bone tibia.

A single dose of 600,000 IU Benzetacil (Eurofarma, São Paulo, Brazil) was used in animals related to the weight of animals. After the surgeries, the animals were housed in their own cages, with special care from a veterinarian, with diet ad libitum, soft glucose-free and kept at a temperature of $21\text{ }^{\circ}\text{C}$

inside the cage. Six weeks after the implantations, all animals were sacrificed through an intravenous overdose of ketamine 2 mL (Agener Pharmaceutica, São Paulo, Brazil) and xylazine 1 mL (Bayer, São Paulo, Brazil). The tibias were removed and placed in 10% formalin solution and kept for one week for fixation.

Removal torque test: Both tibias of the lot of five animals, previously designed for the biomechanics test, were removed and processed immediately after the euthanasia for the measurement of the maximum removal torque of each implant to conserve the mechanical proprieties of the bone [25]. A similar procedure compared to other studies was performed by our group [26]. The removal torque test was performed using a computerized torque machine (CME, Técnica Industrial Oswaldo Filizola, São Paulo, Brazil), and the mean of maximum removal torque value was calculated for each group.

Histomorphological and histomorphometric procedures: The tibia bone blocks of another five animals containing the implants were dehydrated gradually in successive concentrations of alcohol (50%–100%) and embedded in glycol methacrylate resin (Technovit 9100 VLC, Kulzer, Germany) to produce the slice sections, which cut and ground sections that contained the central part of each implant and had a final thickness of 30 μm were produced using a macro cutting and grinding system (Isomet 2000, Buehler, Germany). Then, the sections were stained with picosirius hematoxylin, and histomorphometric analysis was carried out. Finally, the sample was stained with picosirius hematoxylin and analyzed under an optical microscope (Nikon Eclipse E200, Nikon Corporation, Tokyo, Japan).

The histomorphologic analysis was performed around all implants in order to establish the descriptive characteristics of the new bone present after the bone healing (osseointegration). The histomorphometric measurement of bone to implant contact percentage (BIC%) was performed at images with 50–200 times magnification using specific software (ImageJ for Windows, version 6, Research Services Branch, National Institute of Mental Health, Bethesda, MD, USA). The BIC% was calculated after the measurements of the points with the direct bone to implant contact around the implant and subtracted from the total implant perimeter. Moreover, another quantitative parameter measured was the bone volume percentage (BV%), which was determined using the methodology described in other studies [27,28], where the bone around the implant was divided into two zones: the first zone 1 (0–500 μm) and the second zone 2 (500–1000 μm). Figure 4 shows the two zones analyzed.

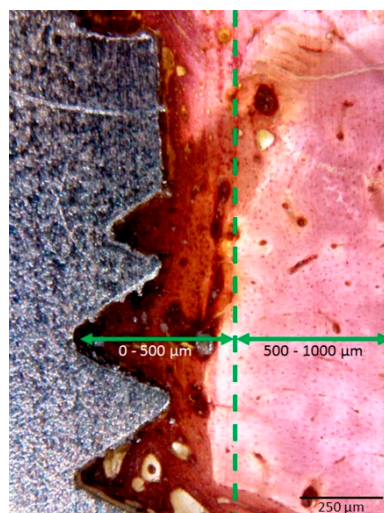


Figure 4. Histological section of the implant in the cortical bone portion (magnification 40 \times) showing 2 zones determined for histomorphometric analysis, which the first zone (0–500 μm) and the second zone (500–1000 μm).

Statistical analysis: The ANOVA One-Way test was used to verify statistical differences among the groups. The comparison between the three groups in the same test was performed using the

Mann-Whitney U-test. These statistical analyses were performed using the software GraphPad Prism 5.01 (GraphPad Software Inc., San Diego, CA, USA). The level of significance was set at $\alpha = 0.05$.

3. Results

3.1. Surface Characterization Analysis

SEM images showed a different surface morphology between the titanium machined surface, titanium treated surface and zirconia implants surface (Figure 1a–c). Table 1 shows the data of roughness parameters (S_a , R_a and Z) of the groups. A highly significant difference in the surface roughness for the TiT group in compare to the TiM and Zr groups for all parameters ($p < 0.0001$).

Table 1. Mean of roughness values S_a and R_a (\pm standard deviation) of both groups.

Parameters	TiM Group	TiT Group	Zr Group
S_a	0.18 (\pm 0.2)	0.77 (\pm 0.2)	0.17 (\pm 0.1)
R_a	0.17 (\pm 0.1)	0.66 (\pm 0.3)	0.14 (\pm 0.2)
Z	0.92 (\pm 0.8)	2.61 (\pm 0.8)	0.77 (\pm 2.0)

S_a = average height of the analyzed area; R_a = arithmetic mean of absolute values of all profile points; Z = longest distance recorded among the peak and valley, high variation of the valleys.

3.2. Removal Torque Test

Table 2 shows the maximum removal torque values measured in the Ti and Zr groups. The values in the Zr group were, on average, half those in the Ti group ($p < 0.0001$). All values measured are presented with the dispersion and median in the graph of Figure 5.

Table 2. Comparison of the maximum removal torque (N cm) between the groups.

Group	Mean	SD	Median	Min	Max	n
TiM	15.9	4.18	16.1	8.4	22.1	10
TiT	27.9	5.15	27.9	15.1	35.3	10
Zr	11.5	2.92	11.1	7.3	16.0	10

SD, standard deviation. Min, minimum value. Max, maximum value. n , number of samples.

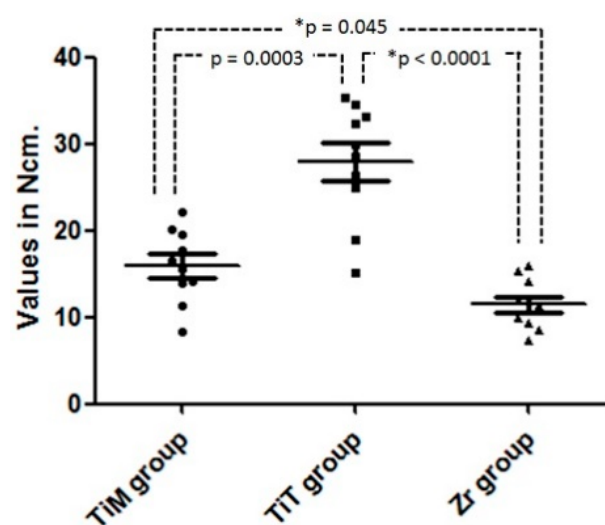


Figure 5. Graph of the removal torque dispersion values and statistical comparison of the groups.

* Statistically difference ($p < 0.05$).

3.3. Histomorphological Analysis

Qualitative evaluation of the histological slides demonstrated that the most cervical portion of all implants passed through the tibial cortical bone, and the apical portion was in contact with medullary bone (Figure 6).

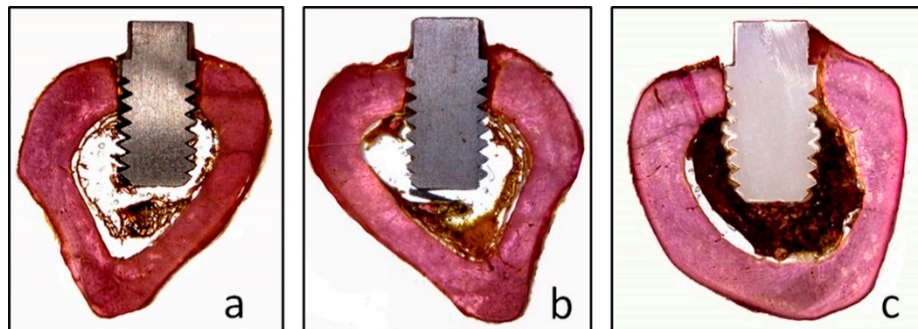


Figure 6. Images of the implants installed in the tibia of the three groups, (a) TiM group, (b) TiT and (c) Zr group.

In the TiM group, a new bone formation was founded in different areas close to the implant surface, with regions of bone remodeling, similar to lamellar bone close to the implant, a large number of voluminous osteocytes was observed located within wide gaps. Moreover, immature bone trabeculae with large remodeling areas were observed. The difference in color staining (more intensely stained areas) showed more new formed bone, founded particularly in between the implant threads (Figure 7).

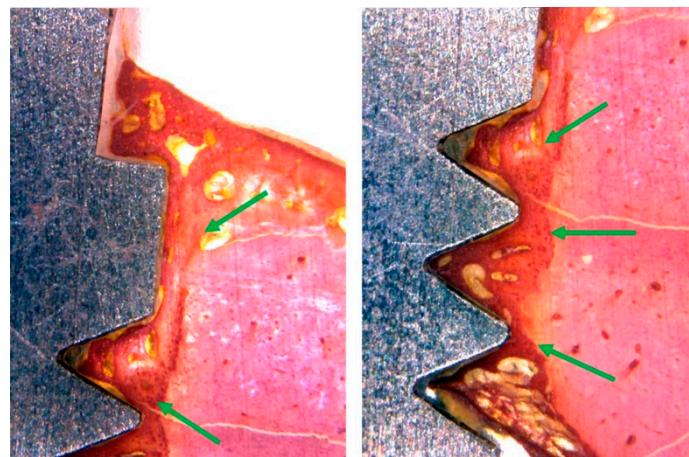


Figure 7. Representative histological images of the TiM group shows the bone to implant contact and a great quantity of bone matrix formation (red staining) around the surface (green arrows).

Whereas, in the TiT group, similar to the TiM group, the histological analysis showed bone neoformation in the areas adjacent to the implant surfaces, with regions of bone remodeling, showing evidence of a structural arrangement similar to that of the lamellar region. Around the implants, a superior bone density was observed and a minimum gap in the interface between bone and implant, with a smaller amount of collagen matrix present in these areas (Figure 8).

However, in the histological analysis of Zr group samples, showed a presence of bone neoformation in the areas adjacent to the implant surfaces, with sites of bone remodeling close to the tops of the spirals and in the more cervical portion of the implant. In some samples, extensive areas of collagen non-mineralized tissue were observed in contact with the implant surface (Figure 9).

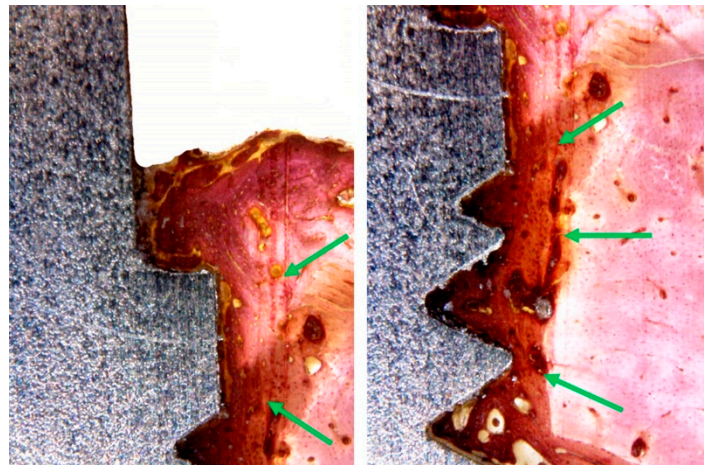


Figure 8. Histological images of the TiT group shows the bone to implant contact and a great quantity of bone matrix formation (red staining) around the surface (green arrows).

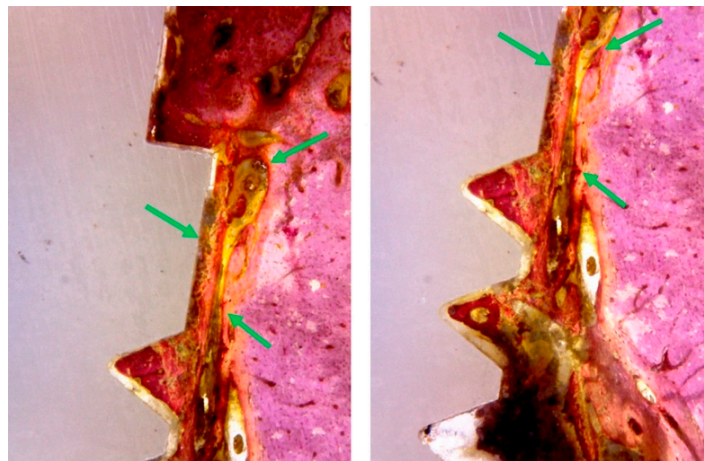


Figure 9. Histological images of the Zr group shows the bone to implant contact and the presence of collagen fibers and less intense density of the bone tissue around the surface (green arrows).

3.4. Histomorphometric Analysis

The mean BIC% values in the Ti group were similar to the values of Zr group, showing no statistically significant difference among the groups (Table 3). The distribution of the BIC% values measured is presented in the box plots graph of Figure 10.

Table 3. Comparison of the bone-implant contact (%) between the groups.

Group	Mean	SD	Median	Min	Max	N
TiM	35.4	4.54	37.1	28.9	41.3	10
TiT	37.8	4.84	39.9	29.8	46.1	10
Zr	34.0	6.82	36.8	23.6	44.0	10

SD, standard deviation. Min, minimum value. Max, maximum value. *n*, number of samples.

The groups showed significant differences in BV% ($p = 0.0012$) for the first zone evaluated (0–500 μm): 51% \pm 6% for TiM group, 77% \pm 5% for TiT group and 42% \pm 5% for Zr group. In the second zone analyzed (500–1000 μm) all samples of the three groups showed a similar BV% with a mean superior to 90%, with no statistical differences ($p > 0.05$).

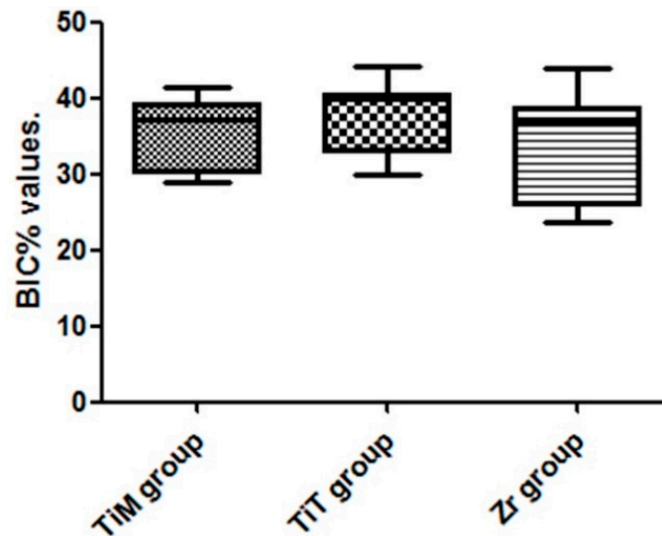


Figure 10. Box-Plot graph of the BIC% values of both groups.

4. Discussion

The goal of this study was to compare the performance of aspects related to osseointegration of titanium (treated and not) and zirconia implants inserted in tibias of rabbits after a period of 6 weeks. This study analyzed the surface roughness (five implants per group), tested the biomechanical proprieties through the resistance to removal torque (10 implants per group) and, finally, measured the percentage of bone-implant contact and bone volume in two determinate areas (0 to 500 μm and 500 to 1000 μm) by a histomorphological analysis (10 implants per group). The results showed an important difference in the biomechanical test (torque removal) and in the bone volume at the measured area from 0 to 500 μm , but no statistical difference in the bone-implant-contact.

The physic-chemical composition and topography of the material surface implanted in the bone are directly related with the response of this tissue and, consequently, with the characteristics of the new tissue formation around of the material surface [28,29]. The present study showed a strong dense bone tissue response to titanium implants in comparison to zirconia implants after 6 weeks of healing in rabbit bone. Furthermore, the treated surface of the titanium implants showed resistance to removal torque forces superior to smooth surface and zirconia implants. These results can have a direct relationship with the fact related in other studies that showed the lower capacity of adhesion of osteoblasts cells on the zirconia structures in comparison with titanium structures [30].

The measurement of the percentage of bone to implant contact (BIC%) around the implants is considered as a parameter to evaluate the potential of osseointegration and it has been used to compare different implants with different macro- and micro-designs, materials or surface modifications [31,32]. The data obtained in our measurements, with respect to BIC%, showed very similar values between the groups, without statistical differences between the three groups, similar with other studies performed on animals comparing zirconia implants with titanium implants [33]. In this case, when we use only this parameter to determine the osseointegration of a material, it can be affirmed that zirconia is a good material to be used as an implant.

Another important parameter to evaluate the osseointegration is the test of torque removal of implants after different times of waiting for healing. In this way, the higher value on the removal torque can be interpreted as an increase in the bone-implant contact [34]. However, the measured value of the torque to remove the implant is directly related by the bone density (maturation and mineralization). This fact was described by Tabassum et al. (2014), showing that the implants evaluated in a period of 3 weeks after their implantation, even presenting high BIC% values, did not show great implant stability. This fact led the authors to propose the probability that this occurred due to the low calcification of the new bone formed at the interface with the implants [28]. During osseointegration of

the implants, one of the phases is the formation of the bone matrix, which can be observed histologically and considered as “new bone” formed. However, in order for this scar tissue to have the necessary mechanical strength to withstand functional needs, proper mineralization is required, which will determine the strength (strength) of the tissue. Thus, through the difference presented between the histological and biomechanical results, we can deduce that titanium implants produce a much superior stimulus for bone matrix mineralization compared to zirconia implants. Correlating with a clinical scenario, early loads should be avoided on zirconia implants.

Removal torque is a common test for *in vivo* analysis to measure the quality of the bone in contact with the implant surface (osseointegration). Therefore, with the removal torque, it is possible to evaluate the strength of the interaction between the bone and implant surface [35]. Good osseointegration is characterized by high values of removal torques [34]. In view of the results obtained in this study, titanium implants obtained a better osteointegration than zirconia implants after 6 weeks. These results were highly significant, and it is thus concluded that there is an important effect among the groups. This is in accordance with other studies [35]. Results detailed in Table 1 show a bigger average in the removal torque values of 38.3% for the TiM group and 142.6% for the TiT group in comparison with the zirconia implants. Similarly, in the study presented by Gahlert et al. which compared the removal torque values of zirconia implants with titanium implants treated by sandblasted acid technique, the machined zirconia implants showed statistically significant lower values than the titanium implant after 8 weeks, being that the treated titanium implant showing values approximately four times bigger than the machined zirconia implants [36].

The time defeminated at 6 weeks in our study was based on previous studies reported in the revised literature [37–39], which concluded that the remodeling process of the bone-to-implant interface is complete in this time for the rabbit animal model. However, Halldin and coworkers demonstrated that the osseointegration of the implants is directly related to the type of bone, that is, it is distinct in trabecular bone than in cortical bone [40,41]. For this reason, and because of the size of the implants prepared for this experiment, the tibia model was selected where the implants, due to their size, were inserted in cortical bone almost half of their total length.

In accordance with Davies [42], the evaluation of the bone healing around the implant surface can be considered in two directions: (1) contact ossification, where the new bone formed evaluated is in direct contact to the implant surface after the cellular events, which was discussed previously as the bone to implant contact (BIC%); (2) ossification in distance, where the process of bone healing is evaluated since of the implant surface to the native bone of the implanted area, in this study called as bone volume (BV%). To determine the bone volume, in the peri-implant area was performed two lines equidistant (since of the implant to the native bone), in accordance to previous studies [27,28]: zone 1 (0–500 μm) representing the area of contact osteogenesis and, zone 2 (500–1000 μm) representing the transition zone for the native bone. Histomorphometric measurements of the samples revealed that for all three groups, the BV% was smaller in zone 1 as compared to zone 2. This can be explained by areas of bone neoformation where we found several zones with the presence of the collagen matrix. In this sense, the TiT group showed the bigger values of BV% in comparison with the TiM and Zr groups. These results are similar to Scarano et al., that demonstrated in their study that zirconia implants can form a great quantity of newly formed bone as the titanium implants [43]. This means that zirconia implants are highly biocompatible and osteoconductive. However, Hoffman et al. However, demonstrated that the zirconia implants obtained a similar rate of bone formation on zirconia and modified titanium surface with a high amount of bone apposition in all implants at 2 and 4 weeks in New Zealand white rabbits [44].

Moreover, when we evaluated the percentages of the neoformed bone area in the zone 1 and compared quantitatively, the results showed a present bone volume of 21.4% for the TiM group and 83.3% for the TiT group in relation to the Zr group. The highest percentage differences were found when comparing the removal torque between the groups, but they followed the same pattern (TiT group > Ti group), demonstrating a relationship between these two measured parameters.

5. Conclusions

Within the limitations of the present animal study, the bone reaction (healing) around the titanium implants showed a more adequate interaction in comparison with the zirconia implants. In this way, the BIC% measured was very similar between the three groups; however, the torque removal values were superior for the titanium implants, which is related to faster bone mineralization on the titanium surface when compared to the zirconia surface for the proposed time period (6 weeks).

Author Contributions: Conceptualization, S.A.G. and L.P.-D.; Methodology, P.M. and J.M.A.; Software, L.P.-D. and J.A.-J.; Validation, S.A.G., J.C.P.-F. and P.N.D.A.; Formal Analysis, P.N.D.A. and M.P.P.; Investigation, S.A.G. and L.P.-D.; Resources, J.C.P.F. and J.L.C.G.; Data Curation, S.A.G., M.P.P. and J.M.A.; Writing—Original Draft Preparation, P.M. and P.N.D.A.; Writing—Review and Editing, P.N.D.A., J.L.C.-G., J.C.P.-F. and M.P.P.; Visualization, L.P.-D. and M.P.P.; Supervision, J.L.C.-G. and J.M.A.; Project Administration, P.N.D.A. and S.G.; Funding Acquisition, S.A.G. and J.A.-J.

Funding: This research received no external funding.

Conflicts of Interest: The authors declare that they have no conflict of interest.

References

1. Kammermeier, A.; Rosentritt, M.; Behr, M.; Schneider-Feyrer, S.; Preis, V. In vitro performance of one- and two-piece zirconia implant systems for an anterior application. *J. Dent.* **2016**, *53*, 94–101. [[CrossRef](#)] [[PubMed](#)]
2. Han, J.; Hong, G.; Lin, H.; Shimizu, Y.; Wu, Y.; Zheng, G.; Zhang, H.; Sasaki, K. Biomechanical and histological evaluation of the osseointegration capacity of two types of zirconia implant. *Int. J. Nanomed.* **2016**, *11*, 6507–6516. [[CrossRef](#)]
3. Bosshardt, D.D.; Chappuis, V.; Buser, D. Osseointegration of titanium, titanium alloy and zirconia dental implants: Current knowledge and open questions. *Periodontol. 2000* **2017**, *73*, 22–40. [[CrossRef](#)] [[PubMed](#)]
4. Chen, Y.W.; Moussi, J.; Drury, J.L.; Wataha, J.C. Zirconia in biomedical applications. *Expert Rev. Med. Devi.* **2016**, *13*, 945–963. [[CrossRef](#)] [[PubMed](#)]
5. Rosentritt, M.; Hagemann, A.; Hahnel, S.; Behr, M.; Preis, V. In vitro performance of zirconia and titanium implant/abutment systems for an anterior application. *J. Dent.* **2014**, *42*, 1019–1026. [[CrossRef](#)]
6. Wenz, H.J.; Bartsch, J.; Wolfart, S.; Kern, M. Osseointegration and clinical success of zirconia dental implants: A systematic review. *Int. J. Prosthodont.* **2008**, *21*, 27–36.
7. Vechiato-Filho, A.J.; Pesqueira, A.A.; De Souza, G.M.; dos Santos, D.M.; Pellizzer, E.P.; Goiato, M.C. Are zirconia implant abutments safe and predictable in posterior regions? A systematic review and meta-analysis. *Int. J. Prosthodont.* **2016**, *29*, 233–244. [[CrossRef](#)]
8. Hashim, D.; Cionca, N.; Courvoisier, D.S.; Mombelli, A. A systematic review of the clinical survival of zirconia implants. *Clin. Oral Investig.* **2016**, *20*, 1403–1417. [[CrossRef](#)]
9. Cionca, N.; Hashim, D.; Mombelli, A. Zirconia dental implants: Where are we now, and where are we heading? *Periodontol. 2000* **2017**, *73*, 241–258. [[CrossRef](#)]
10. Yildirim, M.; Fischer, H.; Marx, R.; Edelhoff, D. In vivo fracture resistance of implant-supported all-ceramic restorations. *J. Prosthet. Dent.* **2003**, *90*, 325–331. [[CrossRef](#)]
11. Bankoğlu Güngör, M.; Aydın, C.; Yılmaz, H.; Gül, E.B. An overview of zirconia dental implants: Basic properties and clinical application of three cases. *J. Oral Implantol.* **2014**, *40*, 485–494. [[CrossRef](#)]
12. Nkamgeu, E.M.; Adnet, J.J.; Bernard, J.; Zierold, K.; Kilian, L.; Jallot, E.; Benhayoune, H.; Bonhomme, P. In vitro effects of zirconia and alumina particles on human blood monocyte-derived macrophages: X-ray microanalysis and flow cytometric studies. *J. Biomed. Mater. Res.* **2000**, *52*, 587–594. [[CrossRef](#)]
13. Rimondini, L.; Cerroni, L.; Carrassi, A.; Torricelli, P. Bacterial colonization of zirconia ceramic surfaces: An in vitro and in vivo study. *Int. J. Oral Maxillofac. Implant.* **2002**, *17*, 793–798.
14. Kohal, R.J.; Wolkewitz, M.; Tsakona, A. The effects of cyclic loading and preparation on the fracture strength of zirconium dioxide implants: An in vitro investigation. *Clin. Oral Implant. Res.* **2011**, *22*, 808–814. [[CrossRef](#)]
15. Kohal, R.J.; Wolkewitz, M.; Hinze, M.; Han, J.S.; Bächle, M.; Butz, F. Biomechanical and histological behavior of zirconia implants: An experiment in the rat. *Clin. Oral Implant. Res.* **2009**, *20*, 333–339. [[CrossRef](#)]

16. Thoma, D.S.; Benic, G.I.; Muñoz, F.; Kohal, R.; Sanz Martin, I.; Cantalapiedra, A.G.; Hämmerle, C.H.; Jung, R.E. Histological analysis of loaded zirconia and titanium dental implants: An experimental study in the dog mandible. *J. Clin. Periodontol.* **2015**, *42*, 967–975. [[CrossRef](#)]
17. Gahlert, M.; Röhling, S.; Wieland, M.; Sprecher, C.M.; Kniha, H.; Milz, S. Osseointegration of zirconia and titanium dental implants: A histological and histomorphometrical study in the maxilla of pigs. *Clin. Oral Implant. Res.* **2009**, *20*, 1247–1253. [[CrossRef](#)]
18. Sanon, C.; Chevalier, J.; Douillard, T.; Cattani-Lorente, M.; Scherrer, S.S.; Gremillard, L. A new testing protocol for zirconia dental implants. *Dent. Mater.* **2015**, *31*, 15–25. [[CrossRef](#)]
19. Guazzato, M.; Albakry, M.; Ringer, S.P.; Swain, M.V. Strength, fracture toughness and microstructure of a selection of all-ceramic materials. Part II. Zirconia-based dental ceramics. *Dent. Mater.* **2004**, *20*, 449–456. [[CrossRef](#)]
20. Kim, J.W.; Covell, N.S.; Guess, P.C.; Rekow, E.D.; Zhang, Y. Concerns of hydrothermal degradation in CAD/CAM zirconia. *J. Dent. Res.* **2010**, *89*, 91–95. [[CrossRef](#)]
21. Wittneben, J.G.; Gavric, J.; Belser, U.C.; Bornstein, M.M.; Joda, T.; Chappuis, V.; Sailer, I.; Brägger, U. Esthetic and clinical performance of implant-supported all-ceramic crowns made with prefabricated or CAD/CAM zirconia abutments. *J. Dent. Res.* **2017**, *96*, 163–170. [[CrossRef](#)]
22. Gehrke, P.; Johannson, D.; Fischer, C.; Stawarczyk, B.; Beuer, F. In vitro fatigue and fracture resistance of one- and two-piece CAD/CAM zirconia implant abutments. *Int. J. Oral Maxillofac. Implant.* **2015**, *30*, 546–554. [[CrossRef](#)]
23. Att, W.; Kurun, S.; Gerds, T.; Strub, J.R. Fracture resistance of single-tooth implant-supported all-ceramic restorations after exposure to the artificial mouth. *J. Oral Rehabil.* **2006**, *33*, 380–386. [[CrossRef](#)]
24. Pieralli, S.; Kohal, R.J.; Jung, R.E.; Vach, K.; Spies, B.C. Clinical outcomes of zirconia dental implants: A systematic review. *J. Dent. Res.* **2017**, *96*, 38–46. [[CrossRef](#)]
25. Morita, K.; Doi, K.; Oue, H.; Kajihara, S.; Hayashi, K.; Akagawa, Y. Influence of formalin fixation on the implant stability quotient and mechanical characteristics of bone. *Br. J. Oral Maxillofac. Surg.* **2013**, *51*, 550–554. [[CrossRef](#)]
26. Gehrke, S.A.; Marin, G.W. Biomechanical evaluation of dental implants with three different designs: Removal torque and resonance frequency analysis in rabbits. *Ann. Anat.* **2015**, *199*, 30–35. [[CrossRef](#)]
27. Tabassum, A.; Meijer, G.J.; Walboomers, X.F.; Jansen, J.A. Evaluation of primary and secondary stability of titanium implants using different surgical techniques. *Clin. Oral Implant. Res.* **2014**, *25*, 487–492. [[CrossRef](#)]
28. Schouten, C.; Meijer, G.J.; van den Beucken, J.J.; Spauwen, P.H.; Jansen, J.A. The quantitative assessment of peri-implant bone responses using histomorphometry and micro-computed tomography. *Biomaterials* **2009**, *30*, 4539–4549. [[CrossRef](#)]
29. Rocchietta, I.; Fontana, F.; Addis, A.; Schupbach, P.; Simion, M. Surface-modified zirconia implants: Tissue response in rabbits. *Clin. Oral Implant. Res.* **2009**, *20*, 844–850. [[CrossRef](#)]
30. Depprich, R.; Ommerborn, M.; Zipprich, H.; Naujoks, C.; Handschel, J.; Wiesmann, H.P.; Kübler, N.R.; Meyer, U. Behavior of osteoblastic cells cultured on titanium and structured zirconia surfaces. *Head Face Med.* **2008**, *4*, 29. [[CrossRef](#)]
31. Rupp, F.; Liang, L.; Geis-Gerstorfer, J.; Scheideler, L.; Hüttig, F. Surface characteristics of dental implants: A review. *Dent. Mater.* **2018**, *34*, 40–57. [[CrossRef](#)]
32. Gehrke, S.A.; Pérez-Albacete Martínez, C.; Piattelli, A.; Shibli, J.A.; Markovic, A.; Calvo Guirado, J.L. The influence of three different apical implant designs at stability and osseointegration process: An experimental study in rabbits. *Clin. Oral Implant. Res.* **2017**, *28*, 355–361. [[CrossRef](#)]
33. Möller, B.; Terheyden, H.; Açıllı, Y.; Purcz, N.M.; Hertrampf, K.; Tabakov, A.; Behrens, E.; Wiltfang, J. A comparison of biocompatibility and osseointegration of ceramic and titanium implants: An in vivo and in vitro study. *Int. J. Oral Maxillofac. Surg.* **2012**, *41*, 638–645. [[CrossRef](#)]
34. Ivanoff, C.J.; Sennerby, L.; Lekholm, U. Influence of mono- and bicortical anchorage on the integration of titanium implants. A study in the rabbit tibia. *Int. J. Oral Maxillofac. Surg.* **1996**, *25*, 229–235. [[CrossRef](#)]
35. Steigenga, J.; Al-Shammari, K.; Misch, C.; Nociti, F.H., Jr.; Wang, H.L. Effects of implant thread geometry on the percentage of osseointegration and resistance to reverse torque in the tibia of rabbits. *J. Periodontol.* **2004**, *75*, 1233–1241. [[CrossRef](#)]

36. Gahlert, M.; Gudehus, T.; Eichhorn, S.; Steinhauser, E.; Kniha, H.; Erhardt, W. Biomechanical and histomorphometric comparison between zirconia implants with varying surface textures and a titanium implant in the maxilla of miniature pigs. *Clin. Oral Implant. Res.* **2007**, *18*, 662–668. [[CrossRef](#)]
37. Klokkevold, P.R.; Johnson, P.; Dadgostari, S.; Caputo, A.; Davies, J.E.; Nishimura, R.D. Early endosseous integration enhanced by dual acid etching of titanium: A torque removal study in the rabbit. *Clin. Oral Implant. Res.* **2001**, *12*, 350–357. [[CrossRef](#)]
38. Sul, Y.T.; Byon, E.S.; Jeong, Y. Biomechanical measurements of calcium-incorporated oxidized implants in rabbit bone: Effect of calcium surface chemistry of a novel implant. *Clin. Implant. Dent. Relat. Res.* **2004**, *6*, 101–110. [[CrossRef](#)]
39. Slaets, E.; Carmeliet, G.; Naert, I.; Duyck, J. Early cellular responses in cortical bone healing around unloaded titanium implants: An animal study. *J. Periodontol.* **2006**, *77*, 1015–1024. [[CrossRef](#)]
40. Halldin, A.; Jimbo, R.; Johansson, C.B.; Wennerberg, A.; Jacobsson, M.; Albrektsson, T.; Hansson, S. The effect of static bone strain on implant stability and bone remodeling. *Bone* **2011**, *49*, 783–789. [[CrossRef](#)]
41. Halldin, A.; Jimbo, R.; Johansson, C.B.; Wennerberg, A.; Jacobsson, M.; Albrektsson, T.; Hansson, S. Implant stability and bone remodeling after 3 and 13 days of implantation with an initial static strain. *Clin. Implant. Dent. Relat. Res.* **2014**, *16*, 383–393. [[CrossRef](#)]
42. Davies, J.E. Understanding peri-implant endosseous healing. *J. Dent. Educ.* **2003**, *67*, 932–949.
43. Scarano, A.; Di Carlo, F.; Quaranta, M.; Piattelli, A. Bone response to zirconia ceramic implants: An experimental study in rabbits. *J. Oral Implantol.* **2003**, *29*, 8–12. [[CrossRef](#)]
44. Hoffmann, O.; Angelov, N.; Gallez, F.; Jung, R.E.; Weber, F.E. The zirconia implant-bone interface: A preliminary histologic evaluation in rabbits. *Int. J. Oral Maxillofac. Implant.* **2008**, *23*, 691–695.



© 2019 by the authors. Licensee MDPI, Basel, Switzerland. This article is an open access article distributed under the terms and conditions of the Creative Commons Attribution (CC BY) license (<http://creativecommons.org/licenses/by/4.0/>).